Geophysical Research Letters

RESEARCH LETTER
10.1029/2020GL090543

How Does the Tibetan Plateau Dynamically Affect Downstream Monsoon Precipitation?

Jun-Hyeok Son[1,2], **Kyong-Hwan Seo**[1,2], **and Bin Wang**[3]

[1]Research Center for Climate Science, Pusan National University, Busan, South Korea, [2]Department of Atmospheric Sciences, Division of Earth Environmental System, Pusan National University, Busan, South Korea, [3]Department of Atmospheric Sciences, IPRC, University of Hawai'i at Mānoa, Honolulu, HI, USA

Key Points:
- Topographically forced stationary Rossby wave theory well explains the seasonal evolution of the downstream East Asian precipitation
- As the season approaches the summer monsoon period, the monsoonal rainband shifts to the west from the western North Pacific to East Asia
- The subtropical zonal wind impinging on the Tibetan Plateau is a primary factor for the enhancement of meridional wind in the EASM region

Supporting Information:
- Supporting Information S1

Correspondence to:
K.-H. Seo,
khseo@pusan.ac.kr

Citation:
Son, J.-H., Seo, K.-H., & Wang, B. (2020). How does the Tibetan Plateau dynamically affect downstream monsoon precipitation? *Geophysical Research Letters*, *47*, e2020GL090543. https://doi.org/10.1029/2020GL090543

Received 31 AUG 2020
Accepted 11 NOV 2020
Accepted article online 23 NOV 2020

Abstract Recent studies have demonstrated that mechanical effects have a greater contribution to the East Asian summer monsoon (EASM) than thermodynamical effects. However, a theoretical basis for the underlying dynamical mechanism has not been elucidated. The present study shows that topographically forced barotropic Rossby wave theory well explains the seasonal evolution of the monsoonal precipitation and its amplitude and peak location. The subtropical zonal wind impinging on the Tibetan Plateau is a key factor, and the resulting downstream cyclonic and anticyclonic circulation anomalies form a peak zonal geopotential height gradient in between, leading to the development of the meridional wind and the accompanying moisture transport to the EASM region. As the season approaches the summer monsoon period, the peak geopotential height gradient—thus the monsoonal rainband—shifts to the west from the western North Pacific to East Asia. The findings in this study can be applied to subtropical monsoons worldwide.

Plain Language Summary Recent observational and modeling studies have demonstrated that the Northern Hemispheric sole subtropical-midlatitude monsoon occurring downstream of the Tibetan Plateau is controlled by both thermodynamical and dynamical factors. The former involves the land-sea temperature contrast and Tibetan Plateau-related elevated heating, whereas the latter includes the dynamical effects due to the squeezing of the air crossing the Tibetan Plateau, which provides a greater contribution to the East Asian summer monsoon (EASM) than the former effect. However, a theoretical basis for the underlying physical mechanism responsible for the EASM precipitation has not been elucidated. The topographically forced barotropic stationary Rossby wave theory, which corresponds to traditional midlatitude atmospheric wave dynamics with topographical forcing, well explains the seasonal evolution of the downstream East Asian precipitation. The subtropical westerly wind impinging on the Tibetan Plateau and the vertical squeezing of the air result in the downstream cyclonic and anticyclonic circulation flow fields, which leads to the development of the southerly wind in between these anomalies and produces moisture transport to the EASM region.

1. Introduction

The Earth's large-scale atmospheric circulation controls the transport of moisture and modulates the global hydrological cycle. The Hadley circulation is a distinct global-scale meridional overturning circulation, and its downward branch is formed over the subtropics owing to energetic constraints and conservation of angular momentum (Held & Hou, 1980). The most natural adjustment of this sinking motion is the development of the zonally symmetric subtropical high and therefore the related climate at this latitude is expected to be dry (Figure S1 in the supporting information). However, in reality, some countries in the subtropics and midlatitudes experience a large amount of precipitation (Rodwell, 1997; Rodwell & Hoskins, 1996, 2001), and especially the East Asian region has long-lasting rainy periods during boreal summer (Seo et al., 2015). This peculiar East Asian summer climate is due to the current geographical distribution of the ocean, land, and topography. Through the land-sea thermal contrast and the resulting converging and diverging motion, a cyclonic circulation is formed over the warm continent, whereas an anticyclonic circulation anomaly is developed over the ocean during summer.

The combined effects of the Hadley circulation and land-sea thermal contrast with tropical monsoon diabatic heating comprise the basic background state for the East Asian climate (Hoskins, 1996;

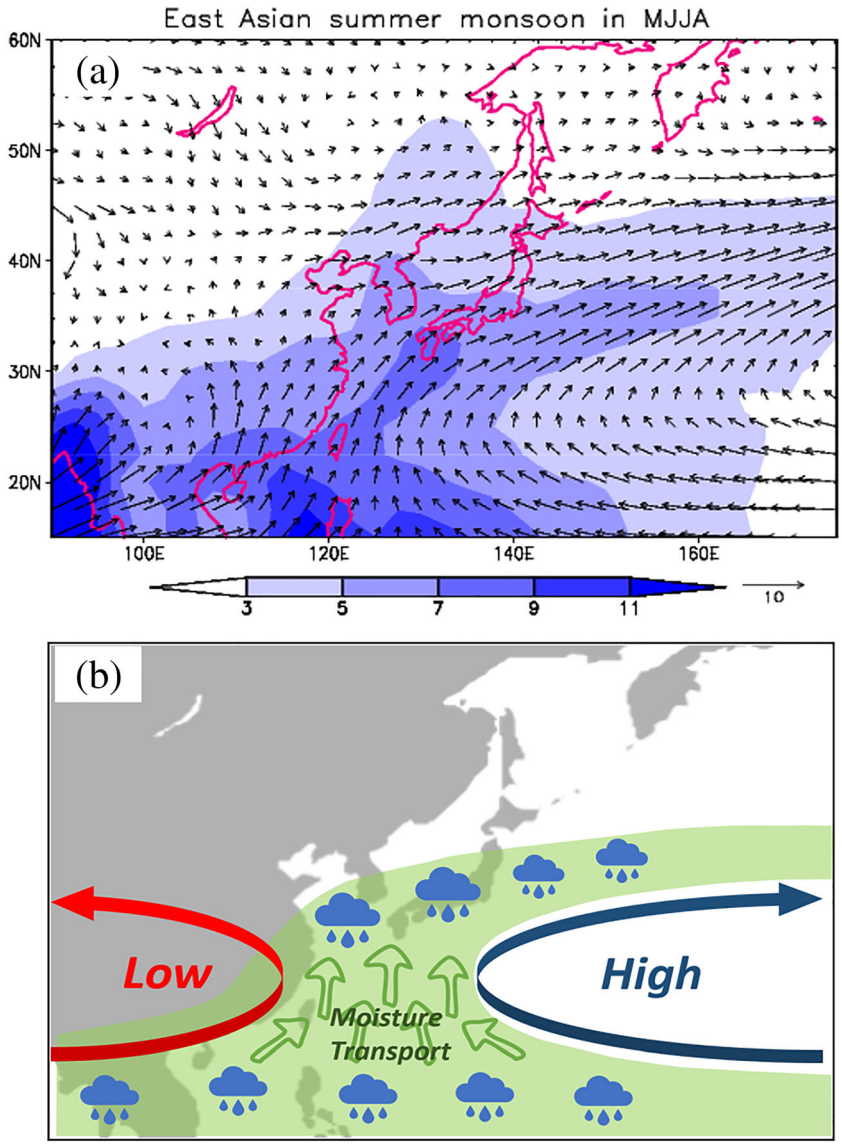

Figure 1. Characteristics of the East Asian summer monsoon (EASM). (a) Climatological mean precipitation and horizontal wind at 850 hPa in boreal summer (May to August) and (b) schematic of the EASM.

Miyasaka & Nakamura, 2005; Rodwell & Hoskins, 2001). Over the land in the subtropics, the cyclonic circulation is formed at lower levels by sensible heat flux and latent heat release, whereas over the ocean, the effect of the land-sea thermal contrast and the stationary Rossby wave response of diabatic heating strengthen the high-pressure system once generated by the downward motion of the Hadley circulation (Figure S2). Thus, it is apparent that this zonally asymmetric pressure pattern is due to the presence of the continents and mountains across the subtropics and midlatitudes.

The most important atmospheric system during this period is the North Pacific subtropical high (NPSH), which is enhanced as it expands to the northwest from winter and spring to summer. Therefore, because East Asia is located in between the pressure low over the land and the NPSH, its summer climate is highly affected by the zonal gradient between the two pressure systems (Figure 1). Thus, the southerly wind along the western edge of the NPSH is one of the key factors in determining the overall characteristics of the East Asian summer monsoon (EASM).

The primary mechanisms of the NPSH formation and development have been previously proposed as follows: elevated heating due to the Tibetan Plateau (which enhances the land-sea heat contrast)

(Wu et al., 2007), downstream Rossby wave circulation response to the continental-scale heat source (Chen et al., 2001; Rodwell & Hoskins, 2001), meridional overturning circulation due to the Pacific ITCZ (Park et al., 2010), zonal overturning circulation response to convective heating over the northern Bay of Bengal and Indian subcontinent (i.e., ITCZ over the Indian monsoon region) (Liu et al., 2004), downstream response of topographically forced Rossby waves (Son et al., 2019), mechanically driven downstream convergence (Kitoh, 2004; Wu et al., 2007), and interactions with the diabatic heating resulting from the downstream response generated mechanically by the Plateau (Biasutti et al., 2018; Miyasaka & Nakamura, 2005). The relative role of all of these possible influences needs to be investigated with carefully designed sensitivity experiments.

Contrary to the traditional understanding regarding the origin of the EASM, which has been assumed to result from the thermodynamical effects due to the land-ocean heat contrast and Tibetan Plateau-induced elevated heating, recent studies have indicated a more crucial role played by mechanical effects due to the existence of the Tibetan Plateau (Abe et al., 2003; Chen & Bordoni, 2014a; Chiang et al., 2015, 2017; Chou et al., 2001; Kitoh, 2004; Molnar et al., 2010; Shaw & Voigt, 2015; Son et al., 2019; Zhang et al., 2018). Uplift over the mountain slope, flow deflection to the north and south of the mountain, and mountain-induced small-scale drag effect are considered as the mechanical effects of the Tibetan Plateau (Son et al., 2019). Among these effects, the effect of mountain drag is assessed to be relatively small (Baldwin & Vecchi, 2016; Cohen & Boos, 2017; Son et al., 2019) and the flow deflection seems to mainly affect the region immediately downstream of the Tibetan Plateau, whereas the flow uplift generates a large-scale circulation response according to the conservation of potential vorticity, and this circulation response is the well-known topographically forced Rossby wave (Charney & Eliassen, 1949; Held, 1983). Valdes and Hoskins (1991) argued that the Tibetan Plateau primarily deflects flow rather than uplifts it, although they suggested that the northern portion of the Tibetan Plateau tends to generate uplift-induced flow. Moreover, recent studies (e.g., Chiang et al., 2015, 2017, 2020) emphasizing that seasonal transitions of the EASM are controlled by the meridional position of the midlatitude westerly jet with respect to the location of the Tibetan Plateau also imply the importance of the deflection effect by the Tibetan Plateau. However, other dynamical effect such as flow uplift may contribute to the development of EASM precipitation. In this study, we demonstrate that the stationary Rossby wave response induced by flow uplift plays a critical role in the generation of the EASM and its zonal evolution. The upstream subtropical westerly winds crossing the Tibetan Plateau experience a change in thickness, which leads to stationary barotropic Rossby waves (Hoskins & Karoly, 1981). These Rossby waves cause the development of a cyclonic circulation to the east of the Tibetan Plateau and an anticyclonic circulation further east. These two pressure anomalies act to generate the southerly wind flow, transporting warm and moist air to the EASM domain (Chang et al., 2000; Chen & Bordoni, 2016; Chou et al., 2009; Seo et al., 2012, 2013; Wang et al., 2013). The advection of heat and moisture from the south induces the confrontation of the different air masses, leading to the formation of the EASM front and therefore precipitation.

The impinging subtropical westerly flow has an apparent annual cycle, with the summer wind being much weaker than that of winter (Figure S3). Here, we demonstrate that this change in the speed of the westerly wind induces a change in the longitudinal location of the ridge and trough of the stationary waves. Consequently, this subtropical westerly flow controls the evolution of the EASM rainband and hydrological cycle through the generation of the downstream Rossby wave.

2. Data Sets and Methods

The Global Precipitation Climatology Project (Huffman et al., 2001) daily precipitation and the European Centre for Medium-Range Weather Forecasts Interim Reanalysis (ERA-Interim) (Dee et al., 2011) products are used. The climatological average for all variables is calculated from 1979 to 2018, except for precipitation (1997–2015). The Earth Topography Five Minute Grid (ETOPO5) data set is downloaded from https://www.ngdc.noaa.gov/mgg/global/etopo5.HTML and interpolated to a 2.5° × 2.5° horizontal resolution for the theoretical prediction of the EASM (National Geophysical Data Center, 1988).

The dynamical response due to orographic forcing can be expressed as the following theoretical solution derived from the potential vorticity conservation equation. Through the midlatitude beta plane approxima-

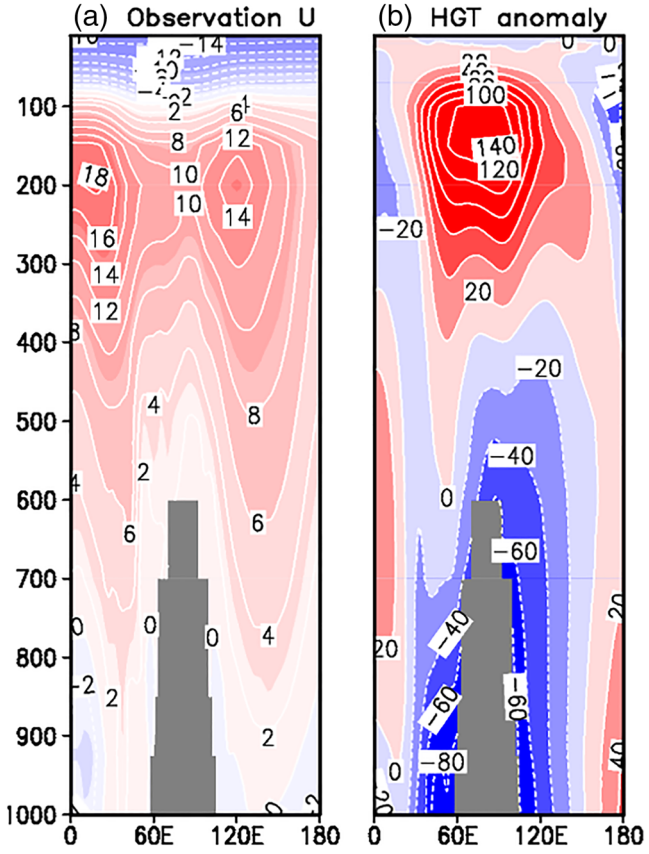

Figure 2. Vertical structure of the atmosphere around the Tibetan Plateau. Vertical and zonal cross section of (a) zonal wind (m s^{-1}) and (b) geopotential height (m), averaged over 25–35°N during May–August. The geopotential height anomaly is calculated by deviations from the zonal average at each pressure level.

tion and introduction of the Rayleigh friction, the forced topographic wave solution (Held, 1983), ϕ_n, is given by

$$\phi_n = \frac{{f_0}^2 h_n}{gH(K^2 - {K_s}^2 - irK^2/k\overline{u})}, \quad (1)$$

where ϕ_n is the geopotential height (m); $f_0 = 10^{-4}$ s^{-1} is the Coriolis parameter; h_n is the topographical height (km); g is the gravitational constant; $H = 8$ km is the scale height; $K^2 = k^2 + l^2$ is the total wavenumber, where $k = \frac{2\pi}{2\pi a \times \cos\left(\frac{latitude}{180}\pi\right) \times n}$ is the zonal wavenumber, $l = \frac{2\pi}{\frac{70}{180}\pi a}$ is the meridional wavenumber (a meridional wave number corresponding to a latitudinal half-wavelength of 35°), and $a = 6{,}371$ km is the Earth radius; ${K_s}^2 = \beta/\overline{u}$ is the stationary wavenumber, $i = \sqrt{-1}$, $r = 1/5$ day^{-1} is the inverse of the spin-down time, and $\overline{u}$ (m s^{-1}) is the zonal wind speed at upper levels measured over the region immediately upstream of the mountain. The forced topographic wave is determined by calculating h_n, using the Fourier transform (Held, 1983). Geopotential height ϕ_n is calculated as a function of only $\overline{u}$ if h_n is prescribed by topography input data and r is fixed.

For a comparison of meridional wind and precipitation between the theoretical solution and observations, an empirical method is used to derive the theoretical meridional wind or precipitation variation. The following formula estimates the fitted slope and intercept:

$$\mathrm{OBS}_{(\text{precipitation or wind})} \sim \alpha \times \mathrm{Theory}_{(\phi_n)} + \beta, \quad (2)$$

where fitting coefficients α and β are obtained by the least squares method.

3. East Asian Summer Climate

The wind direction determines the East Asian weather and climate—the southerly wind prevails in summer, whereas the northerly wind dominates in winter. The change in wind direction during the warm and cold seasons corresponds to the traditional definition of the monsoon (Halley, 1686). These wind changes are accompanied by a variation in precipitation over the monsoon region; during summer, East Asia experiences a massive amount of precipitation.

As mentioned in section 1, the thermodynamical forcing due to the land-sea distribution and elevated terrain contributes to the generation of the EASM; however, the mechanical effects of the Tibetan Plateau are essential for the existence of the EASM (Chen & Bordoni, 2014b, 2016). Among the various mechanical influences of the mountain, the dynamical factor related to the vertical squeezing of the air is the primary source of precipitation formation, which is assessed to account for more than 60% (Son et al., 2019). The Tibetan-Plateau-forced stationary barotropic Rossby wave is conjectured to be a main agent for the enhancement of the NPSH, southerly wind, and monsoonal precipitation.

The topographically forced Rossby wave dynamics can be described by the barotropic stationary wave theory; however, subtropical and midlatitude atmospheric variables, including the westerly jet, do not exhibit a perfectly barotropic structure (Figure 2). Thus, the application of the theory (Equation 1) using the observed field requires a preliminary investigation of the vertical structure and proper consideration of zonal wind forcing. Figure 2a shows that the most vigorous westerly wind (approximately 18 m s^{-1}) appears at 200 hPa over the upstream region of the Tibetan Plateau, and the zonal wind gradually decreases as the height falls. Over the Tibetan Plateau, the westerly wind speed decreases due to mountain drag or the

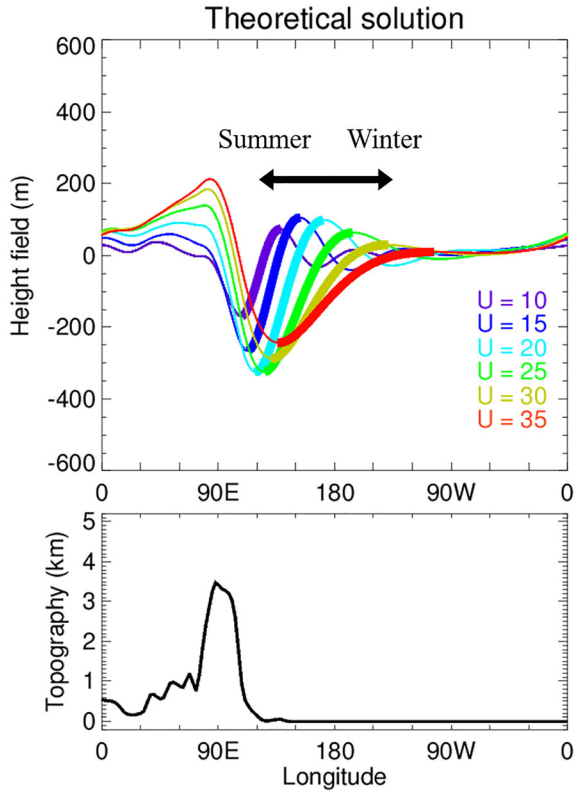

Figure 3. Theoretical prediction of forced topographic wave. The geopotential height response to the zonal wind speeds of 10, 15, 20, 25, 30, and 35 m s^{-1} derived from Equation 1. Thick lines show the maximum pressure gradient regions around East Asia and the western North Pacific. The bottom panel denotes the Eurasian topography (h_n in Equation 1) averaged over 25–35°N.

barrier effect. Recently, the top of the planetary boundary layer over the Tibetan Plateau was discovered to reach up to 300 hPa in spring and early summer (Chen et al., 2013, 2016). Thus, the region slightly west of the Plateau (20–45°E and 500–150 hPa) is selected for the calculation of the impinging westerly wind on the Tibetan Plateau in Equation 1 to minimize the effect of wind deceleration.

Over land, the vertical baroclinic structure is mainly driven by thermodynamic processes (Chen, 2001; Chen et al., 2001; Son & Seo, 2020). The solar radiation warms the surface; then, the thermal energy is transferred to the bottom layer of the atmosphere through sensible and latent heat fluxes (Boos & Kuang, 2013; Hu & Boos, 2017). In the planetary boundary layer, the atmospheric variables have almost uniform physical properties due to turbulent mixing. The thermodynamically driven lower tropospheric warming induces buoyancy and subsequent rising motion, which causes wind convergence, leading to the reinforcement of a cyclonic circulation at the lower layer of the troposphere (Wu et al., 2007, 2012). The upward motion generates the divergent wind and anticyclonic circulation at the upper troposphere. Therefore, the organized convection with the upper-level divergence exports moist static energy away from deep convection to alleviate horizontal energy imbalance (Biasutti et al., 2018). Consequently, the first baroclinic vertical structure around monsoon area is formed through the thermodynamic processes (Figure 2b).

Thus far, the thermodynamically driven heat low has been regarded as the dominant physical mechanism of the cyclonic circulation over the Eurasian continent (Chen, 2001; Chen et al., 2001; Wu et al., 2007, 2012). However, the trough appearing in the eastern part of the continent is affected by the equivalent barotropic Rossby waves. Therefore, the lower-level cyclonic circulation to the east of the Tibetan Plateau is generated by the combination of dynamical (barotropic mode) and thermodynamical (first baroclinic mode) processes. The thermodynamically induced cyclonic circulation is confined inland, whereas the dynamically generated Rossby wave trough can be extended further east, to the western North Pacific.

4. Evolution of the EASM

According to Equation 1, derived from the barotropic Rossby wave theory, the phase and amplitude of the downstream stationary Rossby wave are dependent on the speed of the upstream westerly wind impinging on the mountain. The topography data (h_n) are prescribed as shown in the bottom panel of Figure 3. The upper panel of Figure 3 depicts the geopotential height response to the zonal wind forcing, demonstrating that when the wind speed is weak (purple line in Figure 3), the wave amplitude is also weak, and the positive pressure gradient (low to high pressure) region lies around East Asia (~120°E). As the westerly wind is strengthened, the wave amplitude increases and the peak pressure gradient shifts to the east.

Following the seasonal march of the meridional temperature gradient, the zonal wind impinging on the Tibetan Plateau is stronger in winter and weaker in summer. Similar to this theoretical prediction, the observed climatological rainband lies over East Asia in summer and over the Pacific in winter (Figure 4). In fact, the EASM rainband is tilted from the southwest to northeast along the northwestern boundary of the NPSH. Therefore, the westward propagation of this tilted structure is equivalent to the northward movement of the monsoon rainband. From this characteristic, the rainy period in the local EASM regions begins sequentially. The beginning of the monsoon is often characterized by an abrupt northward shift of the rainband, the so-called "jump," which is likely due to the superposition of various processes—the westward propagation of the rainband associated with the Rossby wave response to the flow forcing due to the Tibetan

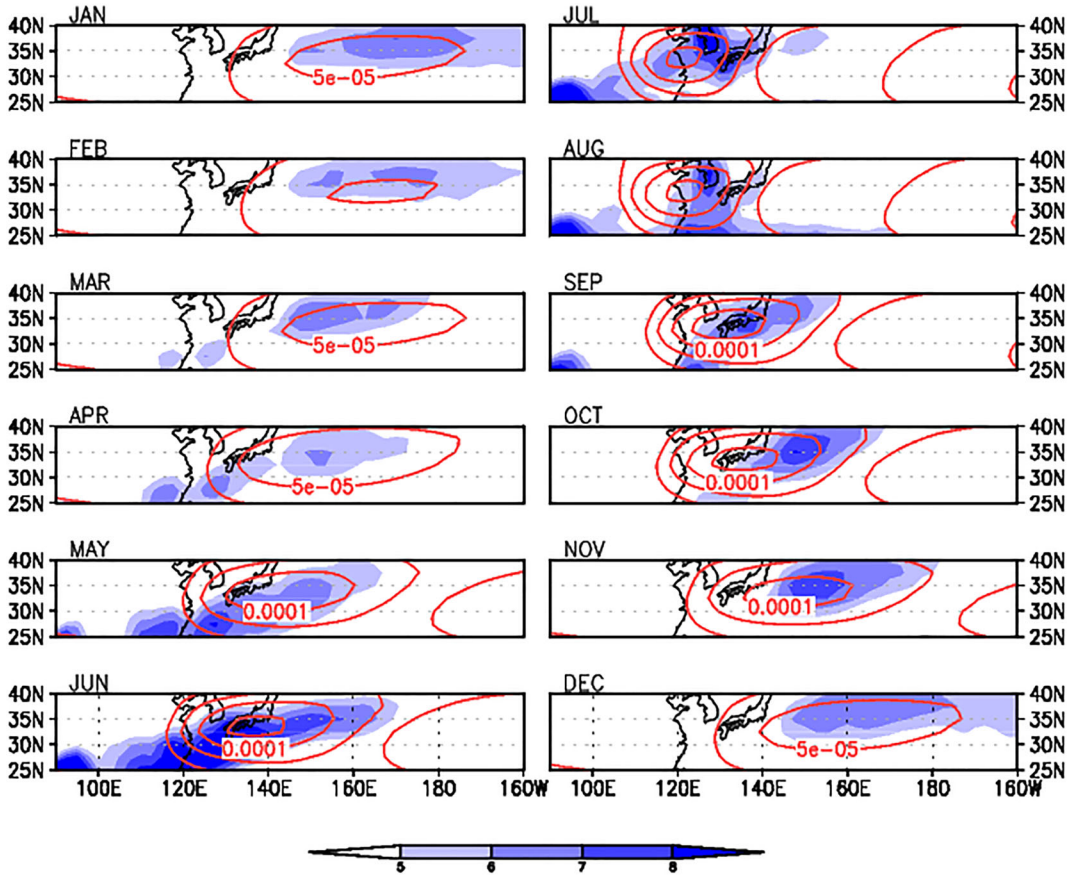

Figure 4. Seasonal evolution of East Asian monsoon precipitation. The climatological evolution of East Asian monsoon precipitation (mm day^{-1}) in observations (blue shading) and the positive zonal gradient of geopotential height ($\partial\phi_n/\partial x$, m km^{-1}) from theoretical predictions (red contour) using the observational upstream zonal wind (20–45°E, 30–35°N, 500–150 hPa).

Plateau, the northward shift of the thermal equator in response to the solar cycle, gradual northward migration of the ITCZ over the Indian monsoon area and its zonal overturning circulation effect, and the increasing land-sea heat contrast during early summer.

Even during fall and winter seasons, the theoretical prediction of the precipitation proxy field is roughly consistent with the evolution of the observed precipitation field (Figure 4). In fact, during winter, even if the baroclinicity is larger and the storm track dynamics are dominant in determining the spatial pattern of precipitation, the topographically induced stationary wave also plays a role in producing additional precipitation.

The prediction of the downstream geopotential height anomalies at the monsoonal latitude using the theoretical derivation (solid line in Figure 5a) matches the observations well (dashed line in Figure 5a). In Figure 5, the discrepancy between the theoretical prediction and observations is thought to be mainly caused by the neglect of topographic forcing by North America and the exclusion of the accurate effect of thermodynamic processes in the theory. Based on Equation 1, the wave response is a function of the zonal wind speed; thus, the geopotential height gradient, which drives the southerly winds, can be plotted against the varying zonal wind speeds measured in the upstream region of the Tibetan Plateau (20–45°E, 25–40°N, 500–150 hPa). In Figure 5c, the zonal gradient of the geopotential height anomaly for the downstream area is calculated by subtracting the averaged geopotential height anomaly for the domain representing the cyclonic circulation anomaly near the land from that representing the anticyclonic circulation anomaly over the ocean. In general, the observed precipitation follows the predicted curve (Figure 5c), with both exhibiting a peculiar convex-shaped structure. This nonmonotonic response results from the zonal phase shift of the

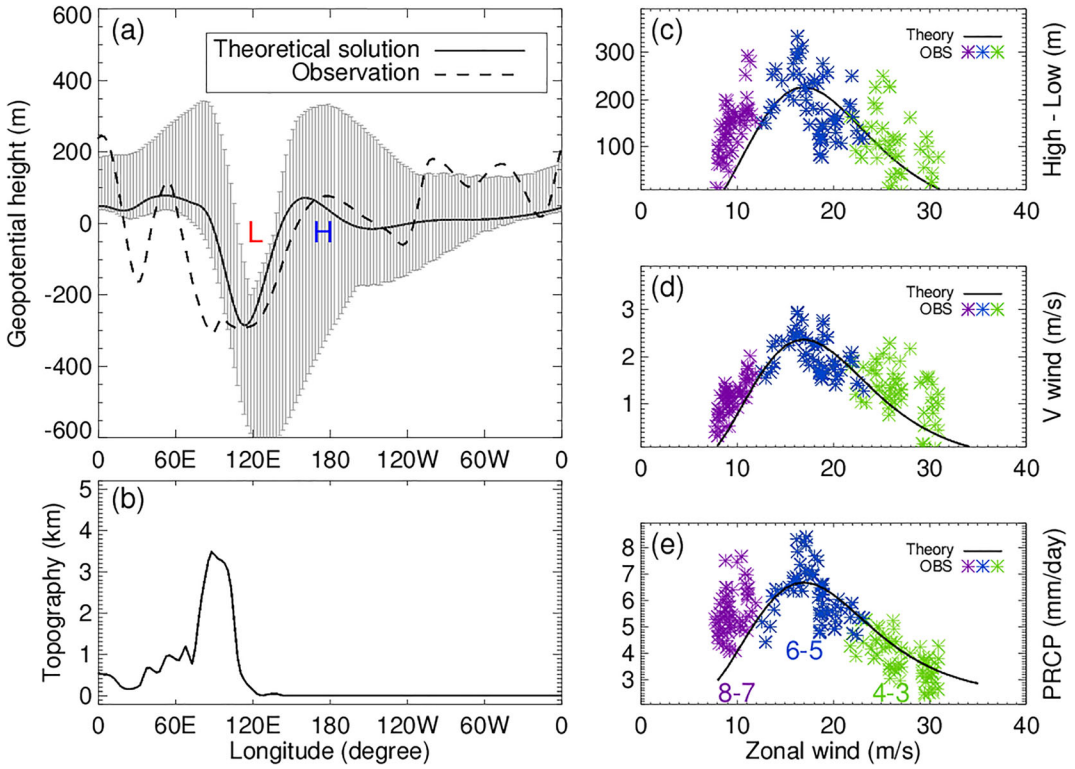

Figure 5. Theoretical prediction and observations of the EASM. Geopotential height anomalies averaged over 25°–35°N from May to July for (a) theoretical prediction (solid line) and observations (dashed line). For observations, the 600–400 hPa averaged geopotential height anomaly (dashed line) is used. The error range is calculated using a damping time scale of 2–8 days and a zonal wind range of 15–30 $m{\cdot}s^{-1}$. (b) The Tibetan Plateau in the Eurasian continent (0–160°E) is used as topographic forcing. Theoretical prediction and observations (daily climatological calendar mean during April to August) of (c) the geopotential height difference (135–150°E, 25–35°N) to (120–130°E, 25–35°N), (d) meridional wind (120–150°E, 25–35°N), and (e) precipitation (120°–150°E, 25°–40°N) for the varying zonal wind speed (20–45°E, 25–40°N, 500–150 hPa). In (e), the numbers 8–7, 6–5, and 4–3 represent the month range.

peak zonal geopotential height gradient due to the seasonal evolution of the subtropical jet stream (Figure 5c). The maximum response appears for a zonal wind speed near 16 m s^{-1}.

Similar to the geopotential height gradient (Figure 5c), both the estimated meridional wind and precipitation (Figures 5d and 5e) exhibit similar profiles to those of the observations. In this case, as no explicit relationship between the meridional wind or precipitation and the zonal wind exists, the geopotential height gradient structure shown in Figure 5c is adopted to fit the observations using Equation 2. From the least squares error method, fitting coefficients have been obtained from observations approximately as $\alpha = 0.01$ and $\beta = 0.23$ for the meridional wind, $\alpha = 0.02$ and $\beta = 3.16$ for the precipitation. The observed meridional wind and precipitation generally follow a simple empirical curve (Figures 5d and 5e). To conclude, the variations of the EASM in circulation and precipitation are consistent with, and appear to be caused by, the Tibetan Plateau-forced Rossby wave dynamics (Figures 5c–5e).

5. Discussion

The change in the monsoonal wind direction modulates the East Asian climate. Thermodynamical and dynamical processes determine the seasonally prevailing wind around East Asia. As the season approaches the summer monsoon period, the rainband propagates to the west, reaching East Asia. This seasonal evolution of the rainband is mainly controlled by the fluid dynamical response to the Tibetan Plateau, with the upstream subtropical westerly wind speed being the key factor. The topographically forced stationary Rossby waves create a downstream zonal pressure gradient and southerly wind, transporting the moisture to East Asia. The present study reveals the fundamental mechanism of the EASM in the climatological sense;

however, its interannual or interdecadal variability needs to be investigated further. The performances of a variety of global climate models can be tested using this theory. The preliminary application of this approach, using the CMIP5 data set, demonstrates that a better simulation of EASM precipitation is achieved if the theoretical prediction is well reflected in the models, which will be reported in a separate study.

Additionally, this study has ramifications for the estimation of the effect of climate change. Under global warming, the subtropical zonal wind is expected to shift northward and weaken (Lorenz & DeWeaver, 2007). If this is the case, the EASM is likely to take place earlier and end earlier, or the main rainfall region would be shifted slightly to the west, according to the above relationship between the geopotential height gradient and upstream zonal wind forcing.

Finally, if the theoretical prediction of the EASM *were* a linear function of the upstream zonal wind speed, then the East Asian climate would experience more dramatic variations in circulation and precipitation; however, the convex-shaped quadratic solution, in reality, leads to a rather stable system. The current theory is expected to serve as a scientific cornerstone for the development of a theoretical framework for the subtropical or midlatitude monsoon system.

Data Availability Statement

The ERA-Interim data were taken online (https://apps.ecmwf.int/datasets/). The GPCP precipitation data were downloaded online (https://www.ncei.noaa.gov/data/global-precipitation-climatology-project-gpcp-daily/access/). The ETOPO5 topography data were taken online (https://www.ngdc.noaa.gov/mgg/global/etopo5.HTML).

Acknowledgments
This work was supported by the National Research Foundation of Korea (NRF) grant funded by the Korea government (MSIP) (NRF-2020R1A2C2009414 and NRF-2020R1I1A1A01061045) and the KMA Research and Development Program under Grant KMI2020–01114. We would like to thank Profs. William Boos and Daehyun Kim for their helpful comments. We are grateful to the reviewers for their valuable comments and suggestions, which improved the paper. All original data sets used in this study are publicly available.

References

Abe, M., Kitoh, A., & Yasunari, T. (2003). An evolution of the Asian summer monsoon associated with mountain uplift—Simulation with the MRI atmosphere-ocean coupled GCM. *Journal of the Meteorological Society of Japan*, *81*(5), 909–933. https://doi.org/10.2151/jmsj.81.909

Baldwin, J., & Vecchi, G. (2016). Influence of the Tian Shan on arid extratropical Asia. *Journal of Climate*, *29*, 5741–5762. https://doi.org/10.1175/JCLI-D-15-0490.1

Biasutti, M., Voigt, A., Boos, W. R., Braconnot, P., Hargreaves, J. C., Harrison, S. P., et al. (2018). Global energetics and local physics as drivers of past, present and future monsoons. *Nature Geoscience*, *11*, 392–400. https://doi.org/10.1038/s41561-018-0137-1

Boos, W., & Kuang, Z. (2013). Sensitivity of the south Asian monsoon to elevated and non-elevated heating. *Scientific Reports*, *3*, 1192. https://doi.org/10.1038/srep01192

Chang, C.-P., Zhang, Y., & Li, T. (2000). Interannual and interdecadal variations of the East Asian summer monsoon and tropical Pacific SSTs. Part I: Roles of the subtropical ridge. *Journal of Climate*, *13*(24), 4310–4325. https://doi.org/10.1175/1520-0442(2000)013<4310:IAIVOT>2.0.CO;2

Charney, J. G., & Eliassen, A. (1949). A numerical method for predicting the perturbations of the middle latitude westerlies. *Tellus*, *1*(2), 38–54. https://doi.org/10.1111/j.2153-3490.1949.tb01258.x

Chen, J., & Bordoni, S. (2014a). Orographic effects of the Tibetan Plateau on the East Asian summer monsoon: An energetic perspective. *Journal of Climate*, *27*(8), 3052–3072. https://doi.org/10.1175/JCLI-D-13-00479.1

Chen, J., & Bordoni, S. (2014b). Intermodel spread of East Asian summer monsoon simulations in CMIP5. *Geophysical Research Letters*, *41*, 1314–1321. https://doi.org/10.1002/2013GL058981

Chen, J., & Bordoni, S. (2016). Early summer response of the East Asian summer monsoon to atmospheric CO_2 forcing and subsequent sea surface warming. *Journal of Climate*, *29*, 5431–5446. https://doi.org/10.1175/jcli-d-15-0649.1

Chen, P. (2001). Thermally forced stationary waves in a quasigeostrophic system. *Journal of the Atmospheric Sciences*, *58*(12), 1585–1594. https://doi.org/10.1175/1520-0469(2001)058<1585:TFSWIA>2.0.CO;2

Chen, P., Hoerling, M. P., & Dole, R. M. (2001). The origin of the subtropical anticyclones. *Journal of the Atmospheric Sciences*, *58*(13), 1827–1835. https://doi.org/10.1175/1520-0469(2001)058<1827:TOOTSA>2.0.CO;2

Chen, X. L., Añel, J. A., Su, Z., de la Torre, L., Kelder, H., van Peet, J., & Ma, Y. (2013). The deep atmospheric boundary layer and its significance to the stratosphere and troposphere exchange over the Tibetan Plateau. *PLoS ONE*, *8*, e56909. https://doi.org/10.1371/journal.pone.0056909

Chen, X. L., Skerlak, B., Rotach, M. W., Añel, J. A., Su, Z., Ma, Y., & Li, M. (2016). Reasons for the extremely high-ranging planetary boundary layer over the western Tibetan Plateau in winter. *Journal of the Atmospheric Sciences*, *73*, 2021–2038. https://doi.org/10.1175/JAS-D-15-0148.1

Chiang, J., Fung, I. Y., Wu, C. H., Cai, Y., Edman, J. P., Liu, Y., et al. (2015). Role of seasonal transitions and westerly jets in East Asian paleoclimate. *Quaternary Science Reviews*, *108*, 111–129. https://doi.org/10.1016/j.quascirev.2014.11.009

Chiang, J., Kong, W., & Battisti, D. (2020). Origins of East Asian summer monsoon seasonality. *Journal of Climate*, *33*, 7945–7965. https://doi.org/10.1175/JCLI-D-19-0888.1

Chiang, J., Swenson, L., & Kong, W. (2017). Role of seasonal transitions and the westerlies in the interannual variability of the East Asian summer monsoon precipitation. *Geophysical Research Letters*, *44*, 3788–3795. https://doi.org/10.1002/2017GL072739

Chou, C., Huang, L.-F., Tseng, L., Tu, J.-Y., & Tan, P.-H. (2009). Annual cycle of rainfall in the western North Pacific and East Asian sector. *Journal of Climate*, *22*(8), 2073–2094. https://doi.org/10.1175/2008JCLI2538.1

Chou, C., Neelin, J. D., & Su, H. (2001). Ocean–atmosphere–land feedbacks in an idealized monsoon. *Quarterly Journal of the Royal Meteorological Society*, *127*(576), 1869–1891. https://doi.org/10.1002/qj.49712757602

Cohen, N. Y., & Boos, W. R. (2017). The influence of orographic Rossby and gravity waves on rainfall. *Quarterly Journal of the Royal Meteorological Society*, *143*, 845–851. https://doi.org/10.1002/qj.2969

Dee, D., Uppala, S. M., Simmons, A. J., Berrisford, P., Poli, P., Kobayashi, S., et al. (2011). The ERA-Interim reanalysis: Configuration and performance of the data assimilation system. *Quarterly Journal of the Royal Meteorological Society*, *137*(656), 553–597. https://doi.org/10.1002/qj.828

Halley, E. (1686). An historical account of the trade winds, and monsoons, observable in the seas between and near the tropics, with an attempt to assign the physical cause of said winds. *Philosophical Transactions of the Royal Society*, *16*, 153–168.

Held, I. M. (1983). Stationary and quasi-stationary eddies in the extratropical troposphere. In B. J. Hoskins & R. P. Pearce (Eds.), *Theory, large-scale dynamical processes in the atmosphere* (pp. 127–168). New York: Academic Press.

Held, I. M., & Hou, A. Y. (1980). Nonlinear axially symmetric circulations in a nearly inviscid atmosphere. *Journal of the Atmospheric Sciences*, *37*(3), 515–533. https://doi.org/10.1175/1520-0469(1980)037<0515:NASCIA>2.0.CO;2

Hoskins, B. (1996). On the existence and strength of the summer subtropical anticyclones. *Bulletin of the American Meteorological Society*, *77*, 1287–1292.

Hoskins, B. J., & Karoly, D. J. (1981). The steady linear response of a spherical atmosphere to thermal and orographic forcing. *Journal of the Atmospheric Sciences*, *38*(6), 1179–1196. https://doi.org/10.1175/1520-0469(1981)038<1179:TSLROA>2.0.CO;2

Hu, S., & Boos, W. R. (2017). The physics of orographic elevated heating in radiative–convective equilibrium. *Journal of the Atmospheric Sciences*, *74*, 2949–2965. https://doi.org/10.1175/JAS-D-16-0312.1

Huffman, G. J., Adler, R. F., Morrissey, M. M., Bolvin, D. T., Curtis, S., Joyce, R., et al. (2001). Global precipitation at one-degree daily resolution from multi-satellite observations. *Journal of Hydrometeorology*, *2*(1), 36–50. https://doi.org/10.1175/1525-7541(2001)002<0036:GPAODD>2.0.CO;2

Kitoh, A. (2004). Effects of mountain uplift on East Asian summer climate investigated by a coupled atmosphere-ocean GCM. *Journal of Climate*, *17*(4), 783–802. https://doi.org/10.1175/1520-0442(2004)017<0783:EOMUOE>2.0.CO;2

Liu, Y., Wu, G., & Ren, R. (2004). Relationship between the subtropical anticyclone and diabatic heating. *Journal of Climate*, *17*(4), 682–698. https://doi.org/10.1175/1520-0442(2004)017<0682:RBTSAA>2.0.CO;2

Lorenz, D. J., & DeWeaver, E. T. (2007). The tropopause height and the zonal wind response to global warming in the IPCC scenario integrations. *Journal of Geophysical Research*, *112*, D10119. https://doi.org/10.1029/2006JD008087

Miyasaka, T., & Nakamura, H. (2005). Structure and formation mechanisms of the Northern Hemisphere summertime subtropical highs. *Journal of Climate*, *18*(23), 5046–5065. https://doi.org/10.1175/JCLI3599.1

Molnar, P., Boos, W. R., & Battisti, D. S. (2010). Orographic controls on climate and paleoclimate of Asia: Thermal and mechanical roles for the Tibetan Plateau. *Annual Review of Earth and Planetary Sciences*, *38*(1), 77–102. https://doi.org/10.1146/annurev-earth-040809-152456

National Geophysical Data Center (1988). *Digital relief of the surface of the Earth, data announcement 88-MGG-02*. Boulder, CO: NOAA.

Park, J. Y., Jhun, J. G., Yim, S. Y., & Kim, W. M. (2010). Decadal changes in two types of the western North Pacific subtropical high in boreal summer associated with Asian summer monsoon/El Niño–Southern Oscillation connections. *Journal of Geophysical Research*, *115*, D21129. https://doi.org/10.1029/2009JD013642

Rodwell, M. J. (1997). Breaks in the Asian monsoon: The influence of Southern Hemisphere weather systems. *Journal of the Atmospheric Sciences*, *54*(22), 2597–2611. https://doi.org/10.1175/1520-0469(1997)054<2597:BITAMT>2.0.CO;2

Rodwell, M. J., & Hoskins, B. J. (1996). Monsoons and the dynamics of deserts. *Quarterly Journal of the Royal Meteorological Society*, *122*(534), 1385–1404. https://doi.org/10.1002/qj.49712253408

Rodwell, M. J., & Hoskins, B. J. (2001). Subtropical anticyclones and summer monsoons. *Journal of Climate*, *14*(15), 3192–3211. https://doi.org/10.1175/1520-0442(2001)014<3192:SAASM>2.0.CO;2

Seo, K.-H., Ok, J., Son, J.-H., & Cha, D.-H. (2013). Assessing future changes in the East Asian summer monsoon using CMIP5 coupled models. *Journal of Climate*, *26*, 7662–7675. https://doi.org/10.1175/JCLI-D-12-00694.1

Seo, K.-H., Son, J. H., Lee, J. Y., & Park, H. S. (2015). Northern East Asian monsoon precipitation revealed by air mass variability and its prediction. *Journal of Climate*, *28*, 6221–6233. https://doi.org/10.1175/JCLI-D-14-00526.1

Seo, K.-H., Son, J.-H., Lee, S.-E., Tomita, T., & Park, H.-S. (2012). Mechanisms of an extraordinary East Asian summer monsoon event in July 2011. *Geophysical Research Letters*, *39*, L05704. https://doi.org/10.1029/2011GL050378

Shaw, T., & Voigt, A. (2015). Tug of war on summertime circulation between radiative forcing and sea surface warming. *Nature Geoscience*, *8*, 560–566. https://doi.org/10.1038/ngeo2449

Son, J.-H., & Seo, K.-H. (2020). Mechanisms for the climatological characteristics and interannual variations of the Guinea coast precipitation: Early summer west African monsoon. *Atmosphere*, *11*, 396. https://doi.org/10.3390/atmos11040396

Son, J.-H., Seo, K.-H., & Wang, B. (2019). Dynamical control of the Tibetan Plateau on the East Asian summer monsoon. *Geophysical Research Letters*, *46*, 7672–7679. https://doi.org/10.1029/2019GL083104

Valdes, P. J., & Hoskins, B. J. (1991). Nonlinear orographically forced planetary waves. *Journal of the Atmospheric Sciences*, *48*(18), 2089–2106. https://doi.org/10.1175/1520-0469(1991)048<2089:NOFPW>2.0.CO;2

Wang, B., Xiang, B., & Lee, J.-Y. (2013). Subtropical high predictability establishes a promising way for monsoon and tropical storm predictions. *PNAS*, *110*, 2635–2640. https://doi.org/10.1073/pnas.1212646110

Wu, G., Liu, Y., He, B., Bao, Q., Duan, A., & Jin, F. F. (2012). Thermal controls on the Asian summer monsoon. *Scientific Reports*, *2*, 404. https://doi.org/10.1038/srep00404

Wu, G., Liu, Y., Zhang, Q., Duan, A., Wang, T., Wan, R., et al. (2007). The influence of mechanical and thermal forcing by the Tibetan Plateau on Asian climate. *Journal of Hydrometeorology*, *8*(4), 770–789. https://doi.org/10.1175/JHM609.1

Zhang, H. B., Griffiths, M. L., Chiang, J. C. H., Kong, W. W., Wu, S. T., Atwood, A., et al. (2018). East Asian hydroclimate modulated by the position of the westerlies during Termination I. *Science*, *362*(6414), 580–583. https://doi.org/10.1126/science.aat9393